Humidification-dehumidification (HDH) technology is a carrier-gas-based thermal desalination technique ideal for application in a small-scale system. However, HDH technology currently has a high cost of water production (about $30/m^3$ of pure water produced). This article describes changes in thermal design that make HDH systems more affordable (< $5/m^3$), including development of thermal design algorithms for thermodynamic balancing via mass extractions and injections and design of a bubble column dehumidifier for high-heat and mass-transfer rates in the presence of large amounts of noncondensable gas. Definition of a novel nondimensional parameter known as the modified heat capacity rate ratio has enabled designs that minimize the imbalance in local driving temperature and concentration differences. A new understanding of heat transfer in bubble column heat exchangers has led to low pressure drop designs (< 1 kPa). In addition, the concept of multistaging the uniform temperature column in several temperature steps has led to highly effective designs (about 90 percent).

Thermal Design of Humidification–Dehumidification Systems for Affordable Small-Scale Desalination

G. Prakash Narayan and John H. Lienhard V

More than a billion people lack access to safe drinking water worldwide (United Nations, 2003), with most of them living in low-income communities. In its millennium development goals, the United Nations (2008) highlights the critical need for impoverished and developing regions of the world to achieve self-reliance in potable water supply. Figure 1 further illustrates this intense water scarcity. For example, in India alone, 200,000 villages and several peri-urban communities lack access to safe potable water (Hammond, 2007). There is a clear need to create a sustainable solution to this problem.

Figure 1. Global physical and economic water scarcity

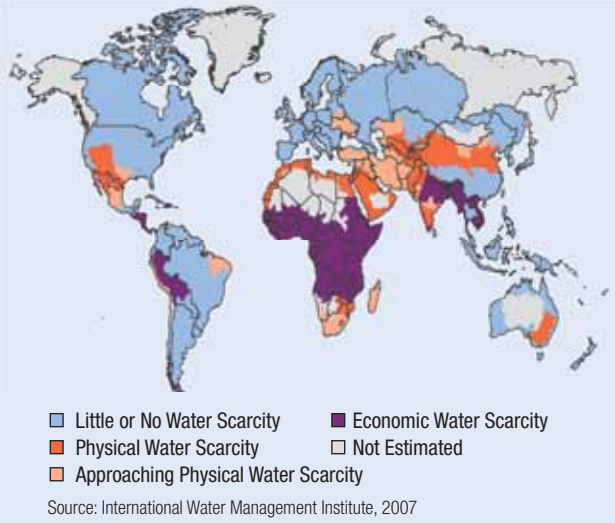

Source: International Water Management Institute, 2007

Most villages lacking safe drinking water are small communities with populations between 1,000 and 10,000 people. Therefore, water for drinking and cooking for each of these communities is about 10–100 m^3 of pure water/day (at a consumption rate of 10 L/person/day). Systems that produce such amounts of pure water are relatively small-scale compared with conventional water treatment systems. For example, most existing state-of-the-art desalination systems produce on the order of 100,000 to 1 million m^3/day (Sauvet-Goichon, 2007).

Need for Small-Scale Desalination Systems

Any potential solution to the problem must be implementable and scalable. In addition, for the solution to be implementable, it must be cost effective and resource frugal. Currently, the price of safe drinking water—in the rare case it is available—in these low-income communities is high relative to the cost of tapped municipal drinking water in nearby developed regions. For example, in some parts of rural India, the cost of water is as high as $\$1/m^3$, which is roughly 40x times the cost of municipal drinking water available in a nearby city (Prahalad and Hammond,

The linchpin in this theoretical work is defining a novel parameter known as the modified heat capacity rate ratio (HCR).

2002). In addition, skilled labor, a continuous energy supply, and raw materials are not readily available in rural areas. The solution must also be implementable within these constraints.

A solution is worthwhile only if it is scalable and can reach a large number of people (a million or more). For such scalability, the solution should be capable of handling an array of contaminants in the water to be treated. In India alone, contaminants range from high fluoride content to bacterial contamination to brackish water.

Fawell et al (2006) reported that 66 million people in India are consuming water with elevated levels of fluoride, most of whom live in the states of Rajasthan and Gujarat where fluoride content is as high as 11 mg/L. Water in some districts in Assam, Orissa, have high iron content (1–10 mg/L, red water). Rajasthan, Uttar Pradesh, and Bihar have yellow water (>1 mg/L of iron) (Bhuyan, 2010). Some places in Haryana, Gujarat, and Andhra Pradesh were also found to have dangerously high levels of mercury. Problems associated with high levels of arsenic in groundwater in West Bengal are well documented (Appello, 2006). In this region, at least 300,000 people are affected by drinking water with arsenic above the permissible limit of 0.05 mg/L. Seawater intrusion in parts of coastal Tamil Nadu has caused high salinity in groundwater (as high as 10,000 ppm in some cases) (Annapoorania et al, 2012). These problems are usually limited to rural and peri-urban communities, with nearly one in three of the 600,000 Indian villages facing problems of brackish or contaminated water and freshwater scarcity.

Distillation-based desalination technologies are known to remove all contaminants, including dissolved ions and micro-organisms. The challenges in implementing these technologies are to do so at low cost (< $\$5/m^3$), at a community scale of 10–100 m^3/day, and be relatively maintenance-free (or capable of being maintained by nontechnical laborers). Humidification–dehumidification (HDH) technology is a carrier-gas-based thermal desalination technique ideal for application in a small-scale system.

HDH Desalination Systems

Nature uses air as a carrier gas to desalinate seawater by means of the rain cycle, in which seawater is heated by solar irradiation and evaporates into the air to humidify it. The humidified air rises and forms clouds. Eventually, the clouds dehumidify as rain over the land, and rainwater can be collected for human consumption. The man-made version of this cycle is called the HDH desalination cycle.

Figure 2 illustrates the simplest form of the HDH cycle. The cycle consists of three subsystems:

Figure 2. Simplest embodiment of HDH process

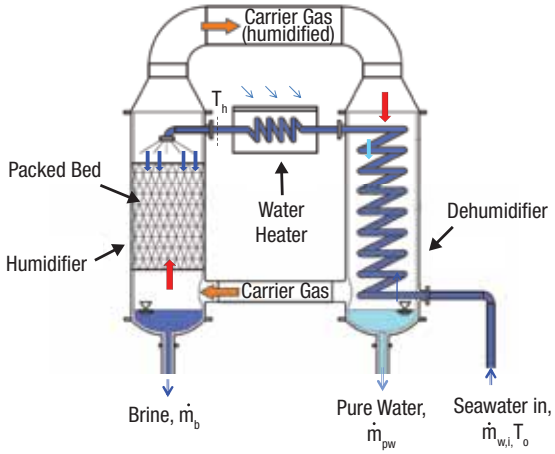

- Air and/or brine heater (only a brine heater is shown in the figure), which can use various sources of heat, such as solar, thermal, geothermal, or combinations of these sources
- Humidifier or evaporator
- Dehumidifier or condenser

The HDH system is ideal for small-scale applications but has two major drawbacks over traditional desalination systems—high thermal energy consumption of 350–550 kW·h/m^3 and heat transfer rates (HTRs), which are two orders of magnitude lower than pure vapor systems. These drawbacks prohibitively increase the cost of water production.

Thermodynamic Balancing in HDH Systems

When finite-time thermodynamics is used to optimize the energy efficiency of thermal systems, the optimal design is one that produces the minimum entropy within the constraints of the problem, such as fixed size or cost. Applying this well-established principle to the thermal design of combined heat and mass exchange devices (dehumidifiers and humidifiers) improves HDH system energy efficiency.

Studies on the effect of entropy generation on HDH system thermal design (Mistry et al, 2011; Miller, 2011) have found that reducing the total entropy generated (per unit amount of water distilled) improves energy efficiency, measured in terms of gained output ratio (GOR). It has also been reported that incorporating mass extractions and injections to vary the water-to-air mass flow rate ratio in the combined heat and mass transfer devices (humidifier and dehumidifier) may help reduce entropy production in those devices (Narayan et al, 2010a). This

Figure 3. Water-heated, closed-air, open-water HDH system with mass extraction and injection of the moist air stream

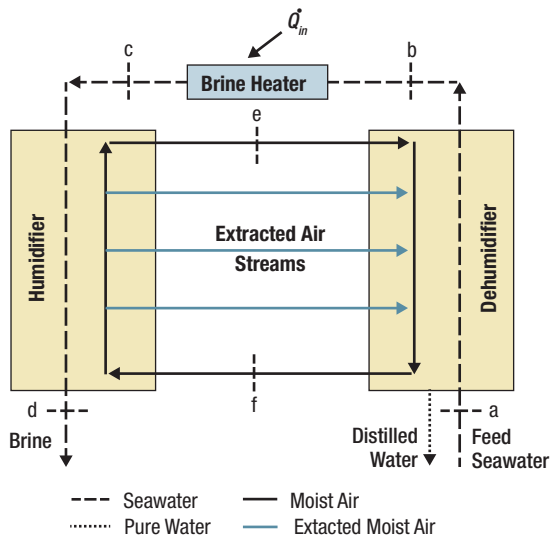

Figure 4. Effect of HCR on entropy generation in a humidifier

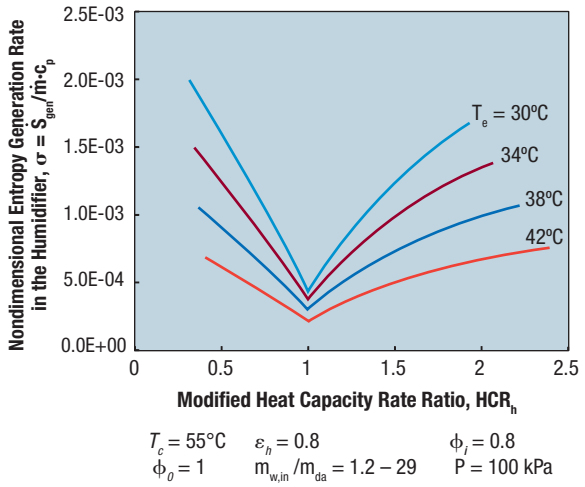

Source: Narayan et al, 2010a

article provides a comprehensive thermodynamic analysis to understand an HDH system's mass extraction and injection design that draws on the fundamental observation that there is a single value of water-to-air mass flow rate ratio for any given boundary conditions and component effectiveness at which the system performs optimally (Narayan et al, 2010b).

Figure 3 shows a diagram of an HDH system with mass extractions and injections. The system shown is a water-heated, closed-air, open-water system with three air extractions from the humidifier into the dehumidifier. States a–d represent various states of the seawater stream and states e and f represent moist air before and after dehumidification. There are several other embodiments of the system possible based on various HDH classifications (Narayan et al, 2010c).

Design Theory. The theoretical design framework for heat-and-mass-exchanger (HME) devices for implementation in an HDH system has been developed in a series of recent papers (Miller, 2011; Narayan et al, 2010a, 2010b, 2010c; Thiel and Lienhard, 2012; Narayan et al, under review). The linchpin in this theoretical work is defining a novel parameter known as the modified heat capacity rate ratio (HCR).

Modified HCR Ratio. In the limit of infinite heat transfer area, the entropy generation rate in a regular heat exchanger will be caused entirely by what is known as thermal imbalance or remanent irreversibility, which is associated with conditions at which the HCR of the streams exchanging heat are not equal (Bejan, 1996). In other words, a heat exchanger (with constant heat capacity for the fluid streams) is said to be thermally balanced (with zero remanent irreversibility) at an HCR ratio of one. This concept of thermodynamic balancing, well known for heat exchangers, was previously extended to HME devices by Narayan et al (2010a).

To define a thermally balanced state in HME devices, a modified HCR for combined heat and mass exchangers was defined by analogy to heat exchangers as the ratio of the maximum change in the total enthalpy rate of the cold stream to that of the hot stream.

Equation 1

$$\mathrm{HCR} = \left(\frac{\Delta \dot{H}_{\max,c}}{\Delta \dot{H}_{\max,b}} \right)$$

The maximum changes are defined by identifying the ideal states that either stream can reach at the outlet of the device. For example, the ideal state that a cold stream can reach at the outlet will match the inlet temperature of the hot stream, and the ideal state that a hot stream can reach at the outlet will match the inlet temperature of the cold stream. The physics behind this definition is explained in detail by Narayan et al (2010a).

As previously illustrated, at fixed inlet conditions and effectiveness, the entropy generation of a combined heat and mass exchange device is minimized when the modified HCR is equal to unity (Narayan et al, 2010a). Figure 4 illustrates this result for a humidifier and shows the nondimensional entropy production as defined by Narayan et al (2010a) plotted against modified HCR ratio

The effect of the number of extractions (at various enthalpy pinches) on HDH system performance was studied using the developed algorithms.

for various values of air inlet temperature at fixed values of energy effectiveness and inlet conditions of air and water streams. Regardless of air inlet temperature, non-dimensional entropy generation is minimized at HCR = 1. This result is true regardless of other fixed condition values.

Further, a recent study (Thiel and Lienhard, 2012) has shown that for a fixed HTR, condensation rate, and HME size, the entropy generation in a dehumidifier approaches a minimum when HCR approaches unity. Miller (2011) developed numerical models to simulate heat and mass transfer in a fixed-area HME device (humidifier and dehumidifier) and reported that, at HCR = 1, the non-dimensional entropy generation is minimized for these devices. Therefore, HCR unity defines the balanced state for HME devices whether it is a fixed-effectiveness or a fixed-hardware condition.

Past work also supports the importance of HCR to the performance of the water-heated HDH system without mass extractions or injections (Narayan et al, 2010b). Figure 5 illustrates the performance variation of the system (gained output ratio or GOR) with the HCR of the dehumidifier (HCR_d). It is apparent that GOR is maximized at HCR_d = 1. The maximum occurs at a balanced condition for the dehumidifier, which is the more irreversible component in this particular cycle.

Therefore, HCR = 1 is the balanced state for HME devices and is the criteria for optimal HDH system performance.

Design Models. HME devices can be studied under the constraint of a fixed performance (with size varying to maintain this performance under varying inlet conditions), known as an on-design analysis, or as a fixed piece of hardware (with varying performance under varying inlet conditions), known as an off-design analysis. Two on-design models developed in previous work (Narayan et al, 2010d; Narayan et al, under review) were reviewed:

- An energy-effectiveness model, which is a control volume-based model
- An enthalpy pinch model, which is used with the knowledge of the process path of the air and water streams.

Effectiveness Model. An energy-based effectiveness model, which is analogous to the effectiveness defined for heat exchangers, is given as:

Equation 2

$$\varepsilon = \left(\frac{\Delta \dot{H}}{\Delta \dot{H}_{max}} \right)$$

Figure 5. HCR of dehumidifier vs. GOR of CAOW water heated HDH system (without mass extractions) at various top brine temperatures

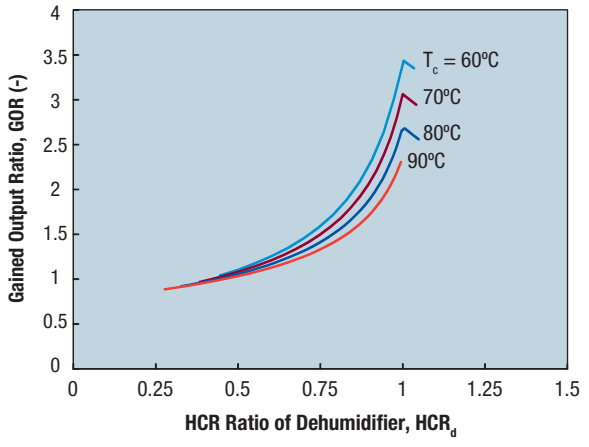

Source: Narayan et al, 2010b

This definition is based on the maximum change in total enthalpy rate that can be achieved in an adiabatic heat and mass exchanger. It is defined as the ratio of change in total enthalpy rate ($\Delta \dot{H}$) to the maximum possible change in total enthalpy rate ($\Delta \dot{H}max$). The maximum possible change in total enthalpy rate can be of the cold or hot stream, depending on the two streams' HCR. The stream with the minimum HCR dictates the thermodynamic maximum amount of heat transfer that can be attained between the fluid streams. This concept is explained in detail by Narayan et al (2010d).

Equation 3

$$\Delta \dot{H}_{max} = \min \left(\Delta \dot{H}_{max,c}, \Delta \dot{H}_{max,h} \right)$$

Enthalpy Pinch Model. McGovern et al (2012 in press) proposed that it is advantageous to normalize enthalpy rates by the amount of dry air flowing through the system for easy representation of the thermodynamic processes in enthalpy vs. temperature diagrams. The authors use this concept here and derive the following equation from Equation 2 by dividing the numerator and the denominator by the mass flow rate of dry air ($\dot{m}da$).

Equation 4

$$\varepsilon = \frac{\Delta b^*}{\Delta b^*_{max}}$$

Equation 5

$$= \frac{\Delta b^*}{\Delta b^* + \Psi_{TD}}$$

Figure 6. Temperature profile of the HDH system with a single extraction

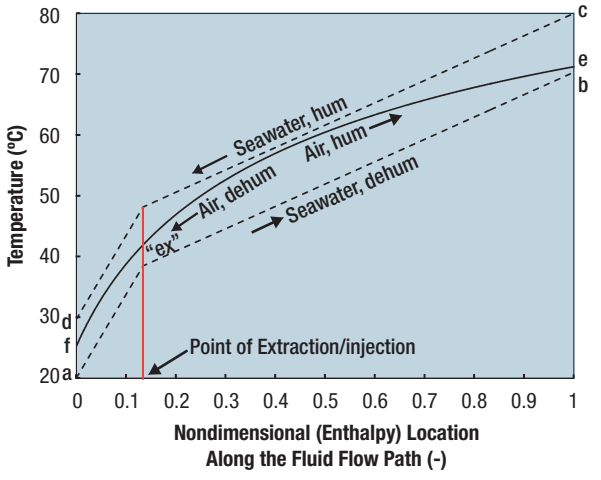

Figure 7. Effect of number of extractions (for thermodynamic balancing) on HDH system performance with finite and infinite size HME devices

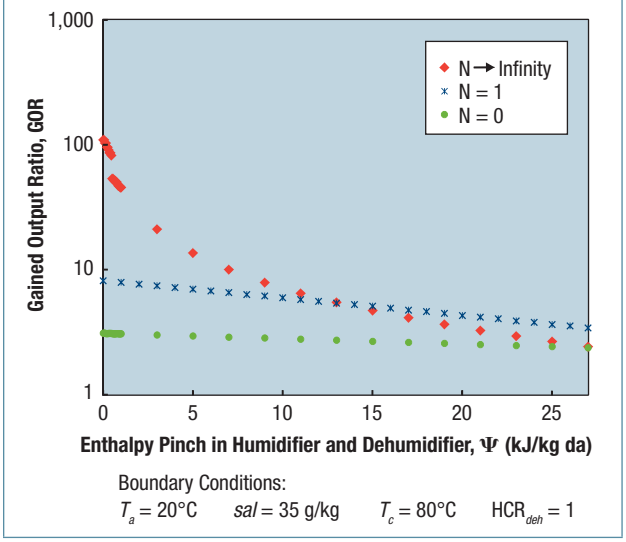

Ψ_{TD} is the loss in enthalpy rates at terminal locations because of having a finite-sized HME device and is defined as follows:

Equation 6

$$\Psi_{TD} = min\left(\frac{\Delta\dot{H}_{\max,c}}{\dot{m}_{da}} - \Delta h^*, \frac{\Delta\dot{H}_{\max,b}}{\dot{m}_{da}} - \Delta h^*\right)$$

Equation 7

$$= min\,(\Psi_c, \Psi_b)$$

In the case of a heat exchanger, Ψ_{TD} will be analogous to the minimum stream-to-stream terminal temperature difference (TTD). TTD is seldom used to define performance of a heat exchanger in thermodynamic analyses; the temperature pinch is the commonly used parameter. The difference is that pinch is the minimum stream-to-stream temperature difference at any point in the heat exchanger, not just at terminal locations. Like temperature pinch, Ψ can be defined as the minimum loss in enthalpy rate due to a finite device size at any point in the HME device, not just at the terminal locations. Therefore, the general definition of Ψ is as follows:

Equation 8

$$\Psi = \min_{local}\,(\Delta h^*_{\max} - \Delta h^*)$$

Based on the arguments presented in this section, Ψ for an HME device is analogous to temperature pinch for a heat exchanger, and it can be called the enthalpy pinch. Because of the presence of the concentration difference as the driving force for mass transfer in HME devices, the authors recommend that a temperature pinch or a terminal temperature difference should not be used when defining the device's performance. Further details about enthalpy pinch and its significance in thermal design of HME devices were provided by Narayan et al (under review).

System Balancing Algorithms. In addition, Narayan (under review) used the concepts of thermodynamic balancing developed for HME devices and applied them to HDH system design. Detailed algorithms for systems with zero, single, and infinite extractions were developed. Temperature-enthalpy diagrams were used to model the systems. Figure 6 illustrates temperature vs. enthalpy of a system with a single extraction and injection. In the illustrated case, the air was extracted from the humidifier at state "ex" and injected in a corresponding location in the dehumidifier with the same state to avoid generating entropy during the injection process. This criteria for extraction is applied for all the cases reported in this article, because it helps to study the effect of thermodynamic balancing, independently, by separating the effects of a temperature and/or a concentration mismatch between the injected stream and the fluid stream passing through the HME device (which, when present, can make it difficult to quantify the reduction in entropy generated by balancing alone).

The effect of the number of extractions (at various enthalpy pinches) on HDH system performance was studied using the developed algorithms and is shown in Figure 7. Several important observations can be made from this chart.

However, by using a bubble column heat (and mass) exchanger, the HTR can be substantially improved by condensing the vapor-gas mixture in a column of cold liquid rather than on a cold surface.

Figure 8. Effect of mass flow rate ratio on nondimensional entropy generation in the humidifier

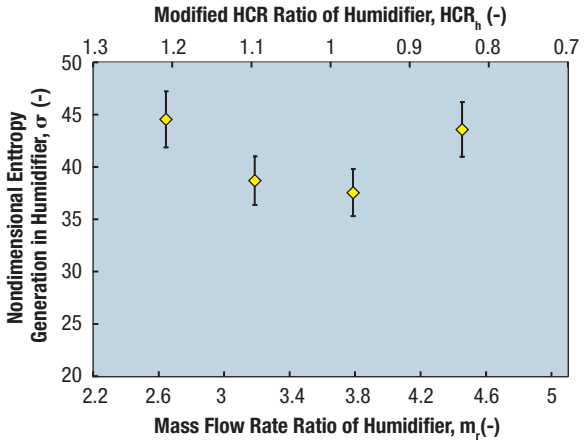

Figure 9. Effect of mass flow rate of air extracted on HDH system performance

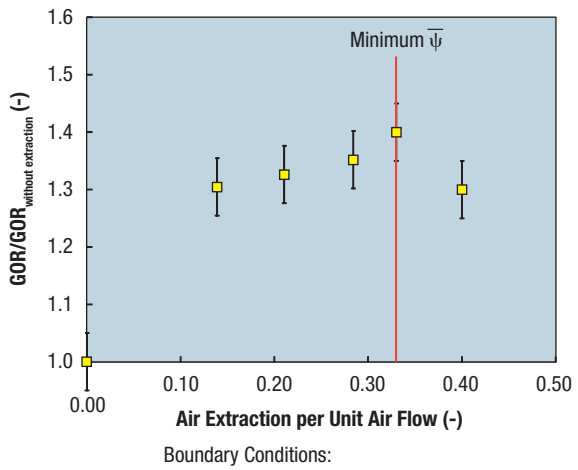

First, it may be observed that thermodynamic balancing is effective in HDH cycles only when the humidifier and dehumidifier have an enthalpy pinch less than about 27 kJ/kg dry air. For various boundary conditions, it has been found that above the aforementioned value of enthalpy pinch the difference in performance (GOR) with that of a system without any extractions or injections is small (less than 20 percent). Further, at very low values of the enthalpy pinch ($\Psi \leq 7$ kJ/kg dry air) in the humidifier and dehumidifier, the limiting case of continuous balancing with infinite number of extractions and injections yielded much better results than a single extraction and injection yielded. For the top brine temperature of 80°C, a feedwater temperature of 20°C, and infinitely large humidifier and dehumidifier ($\Psi_{hum} = \Psi_{deh} = 0$ kJ/kg dry air), GOR was found to be 8.2 for a single extraction (compared with a GOR of 109.7 for a similar system with infinite extractions). At higher values of enthalpy pinch ($7 < \Psi \leq 15$), a single extraction reduced the entropy generation of the total system by a similar amount as continuous extractions. At even higher enthalpy pinch values ($15 < \Psi \leq 27$), a single extraction outperforms continuous extractions.

Experimental Results. A pilot-scale HDH unit producing up to 700 L of pure water/day was built. The unit was fully instrumented, and component and system experiments were carried out on the system.

HME Balancing. As described, theoretical considerations show that a modified HCR of 1 will lead to minimum entropy generation in a fixed-effectiveness or fixed-hardware device (Miller, 2011; Narayan et al, 2010d), and the condition should be established to optimize the HDH cycle's thermal performance (Narayan et al, 2010b).

Figure 8 illustrates a particular mass flow rate at which nondimensional entropy generated in the device is minimized at fixed inlet air condition and fixed inlet water temperature. At different boundary condition values, the same result was found. The observed minimum also corresponds to the case closest to an HCR of 1, which is consistent with the theoretical observation that irreversiblity is minimized at HCR of unity (Miller, 2011; Narayan et al, 2010a; Thiel and Lienhard, 2012).

System Balancing. Figure 9 illustrates the effect of mass flow rate extracted on the increase in performance of the HDH system. The increase in performance of the HDH system is calculated as the ratio of GOR with extraction to that without extraction. In "with" and "without" extraction cases, the top brine temperature, feedwater temperature, water flow rate, and total air flow entering the humidifier from the dehumidifier (measured at state f in Figure 2) are fixed. In the zero extraction case, the ratio is 1 and increases with better balancing. The amount of air extracted is also normalized against total air flow.

It may be observed that performance is optimal at a particular amount of extraction. In this case, when the top temperature is 90°C and the feed temperature is 25°C, the optimum amount of extraction is about 33 percent. GOR is enhanced by up to 40 percent. The trends are similar at different boundary conditions, and the maximum GOR enhancement with a single extraction of air was found to be about 55 percent.

Figure 10. Bubble column dehumidifier

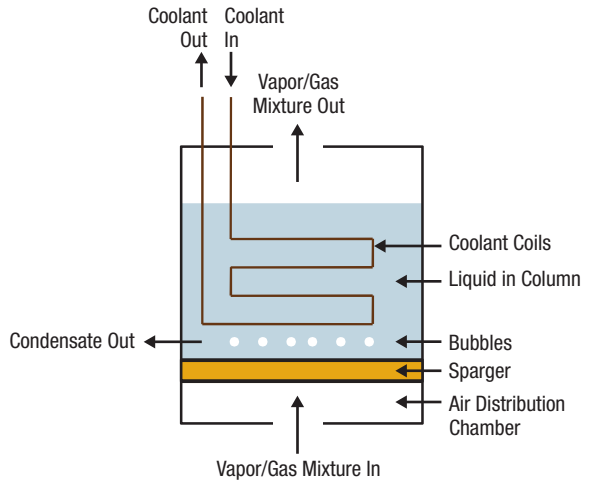

Figure 11. Effect of inlet mole fraction of the vapor on the total heat flux in the bubble column

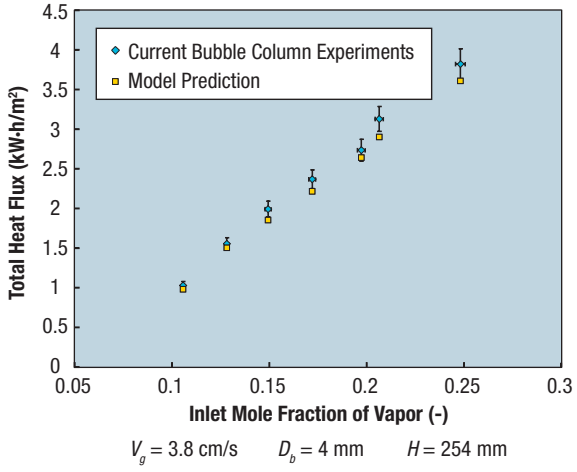

As expected, maximum performance corresponded to the minimum average of local enthalpy pinches in the dehumidifier ($\overline{\Psi}_{local,d}$), which is consistent with the principal purpose of thermodynamic balancing—to drive the process at minimum driving force and correspondingly smaller entropy generation at a fixed system size.

Bubble Column Dehumidification in HDH Systems

When a noncondensable gas is present, the thermal resistance to vapor condensation on a cold surface is much higher than in a pure vapor environment, primarily because of diffusion resistance to transport vapor through the noncondensable gas and vapor mixture. Several researchers have previously studied and reported this effect (Colburn and Hougen, 1934; Nusselt, 1916; Sparrow and Eckert, 1961; Sparrow et al, 1967; Minkowycz and Sparrow, 1966; Denny et al, 1971; Denny and Jusionis, 1972; Wang and Tu, 1988; Kageyama et al, 1993). There is a general consensus that, when even a few mole percent of noncondensable gas is present in the condensing fluid, the deterioration in HTRs could be as much as an order of magnitude (Hasanein, 1994; Kuhn, 1995; Maheshwari et al, 2007; Hasanein et al, 1996; Siddique et al, 1992; Rao et al, 2008). Based on previous experiments and published literature, it can be observed that the amount of deterioration in heat transfer is a strong (almost quadratic) function of the mole fraction of noncondensable gas present in the condensing vapor.

In HDH systems, a large percentage of air (60–90 percent by mass) is present by default in the condensing stream. Consequently, it has been found that the heat exchanger (dehumidifier) used for condensation of water out of an air-vapor mixture has low heat and mass transfer rates, an equivalent heat-transfer coefficient as low as 1 W/m^2 K in some cases (Hamieh et al, 2001; Hamieh and Beckman, 2006; Sievers, 2010). This leads to high heat-transfer area requirements in the dehumidifier (up to 30 m^2 for a 1 m^3/day system). However, by using a bubble column heat (and mass) exchanger, the HTR can be substantially improved by condensing the vapor-gas mixture in a column of cold liquid rather than on a cold surface.

In this device, moist air is sparged through a porous plate, or any other type of sparger (Kulkarni and Joshi, 2011) to form bubbles in a pool of cold liquid, as shown in Figure 10. The upward motion of air bubbles causes a wake to be formed underneath the bubble, which entrains liquid from the pool, setting up a strong circulation current in the liquid pool (Joshi and Sharma, 1979). Heat and mass are transferred from the air bubble to the liquid in the pool in a direct contact transport process. At steady state, the liquid, in turn, loses the energy it gained to the coolant circulating through a coil placed in the pool for the purpose of holding the liquid pool at a steady temperature.

Modeling and Experimental Validation. Narayan et al (2012) developed a thermal resistance model for the condensation of water from an air-vapor mixture in a bubble column heat exchanger. The four temperature nodes in the network are

- the average local temperature of the air-vapor mixture in the bubbles (T_{air}).
- the average temperature of the liquid in the pool (T_{column}).
- the local temperature of the coil surface (T_{coil}).

This innovation reduces the heat-transfer area requirement to a fraction of that in existing HDH systems and is brought close to pure vapor levels.

Figure 12. Multistage bubble column dehumidifier

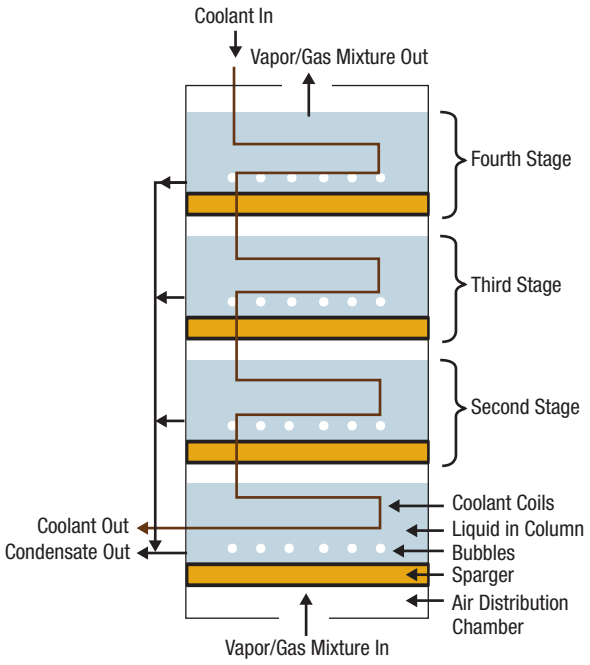

Figure 13. Temperature profile in the bubble columns for (a) single stage and (b) multistage

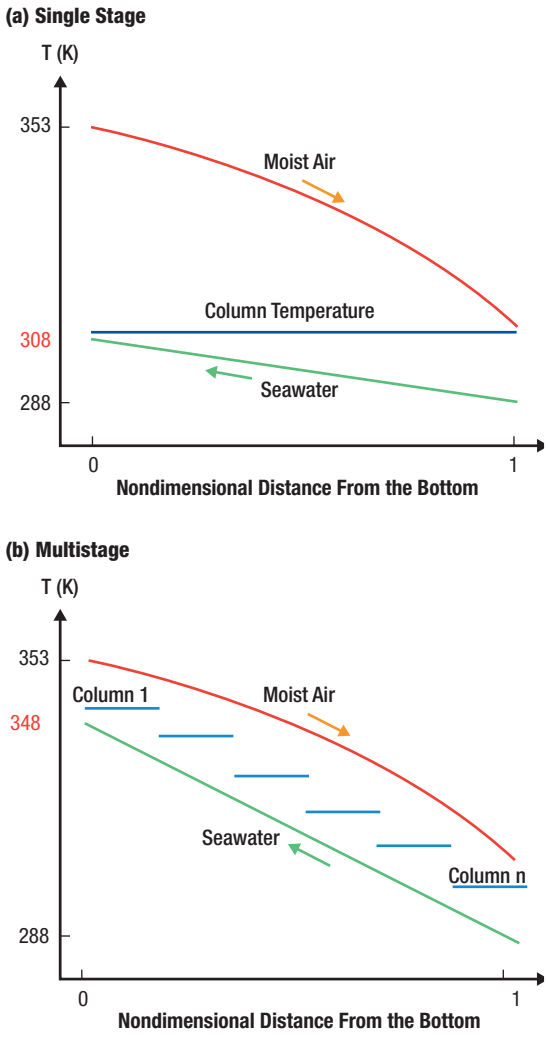

- the average local temperature of the coolant inside the coil ($T_{coolant}$).

Between T_{air} and T_{column}, there is direct contact heat and mass transfer. The heat transfer is via a thermal resistance represented by $R_{sensible}$, and the mass transfer is represented as a latent heat source ($q_{lt} = j \cdot h_{fg}$). There could be direct-contact heat exchange and associated condensation of vapor on the coil surface between the coil surface and the bubble. The heat transfer is via a heat transfer resistance R_{impact} and the mass transfer, represented by the heat source $q_{lt,impact}$. Narayan et al (2012) present further details of the model.

Figure 11 illustrates the experimental and modeling results. A strong effect of the mole fraction is seen, as is the case in steam condensers. From these experiments, the authors observe that the effect is more linear than quadratic (in the studied range). Therefore, the presence of noncondensable gas affects the heat transfer to a much lesser degree than in the film condensation situations of a standard dehumidifier. This demonstrates the superiority of the bubble column dehumidifier (Narayan et al, 2011). Figure 11 also illustrates that the predictive model accurately predicts the effect of inlet mole fraction.

Prototype. In a HDH system, the isothermal nature of the liquid in the bubble column dehumidifier reduces the temperature to that at which seawater can be preheated (in the coils), limiting the device's energy effectiveness (Narayan et al, 2010d). Low effectiveness in the dehumidifier reduces HDH system performance significantly (Narayan et al, 2010b).

A diagram of a multistage bubble column is shown in Figure 12. In this device, the moist air is sparged successively from the bottom-most (first) stage to the top-most (last) stage via a pool of liquid in each stage. The coolant enters the coil in the last stage and passes through the coil in each stage and leaves from the first stage. The condensate is collected directly from the column liquid in each stage.

Figure 13 illustrates temperature profiles in a single stage and multistage bubble column. In both cases, the moist air enters fully saturated at a temperature of 353 K

Figure 14. Effect of mulitstaged bubble column on device's energy effectiveness

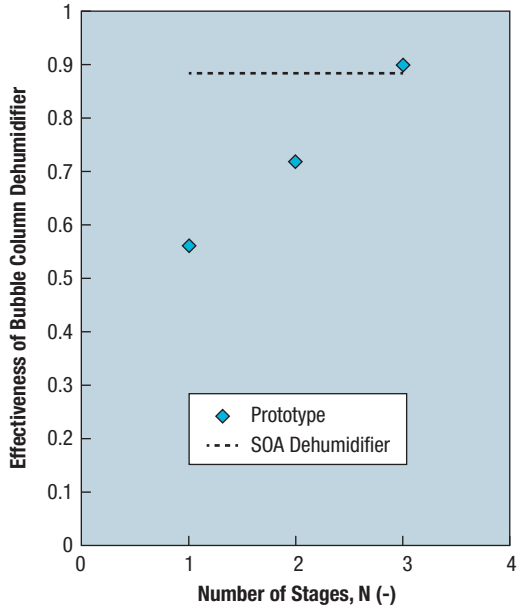

Figure 15. Dehumidifier area requirement for bubble columns compared with existing technology

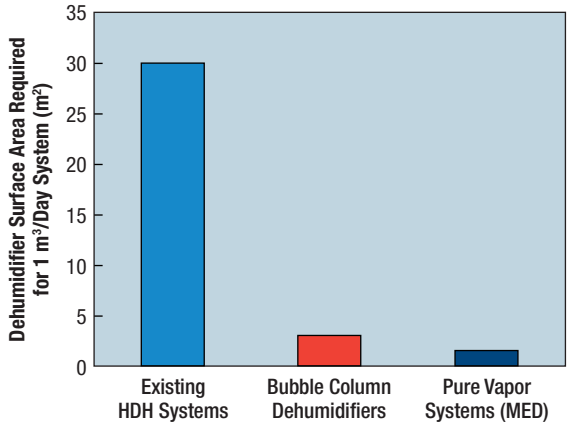

and leaves dehumidified at 310 K. In the process, the pool of liquid in the bubble column gets heated and preheats the seawater going through the coil. In the single-stage case, the coolant gets preheated to a temperature of only 308 K (limited by the air exit temperature of 310 K). This corresponds to a very low effectiveness (30 percent). In the case of multistage bubble columns, the column liquid in each stage is at a different temperature, limited by the temperature of the air passing through the respective stage. Therefore, the outlet coolant temperature is limited only by the exit temperature of the air from the first stage. In this example, the temperature reaches 348 K (40 K higher than the single-stage case), corresponding to an effectiveness increase from 30 percent in the single stage to 92 percent in the multistage.

Figure 14 illustrates the device's increase in effectiveness with multistaging. The data presented here is for an air inlet temperature of 65°C, inlet relative humidity of 100 percent, a water inlet temperature of 25°C, and a water-to-air mass flow rate ratio of 2.45. The device's energy effectiveness is increased from about 54 percent at single stage to about 90 percent for the three-stage device. Further, owing to the higher superficial velocity (because of smaller column diameter), the heat fluxes were much higher (up to 25 kW/m^2) than film-condensation dehumidifiers. Also, the device's total gas-side pressure drop was 800 Pa.

Comparison With Existing Devices. A state-of-the-art dehumidifier[1] that operates in the film condensation regime yielded a maximum heat flux of 1.8 kW/m^2, as per the design specification, compared with the bubble column humidifier's maximum 25 kW/m^2, demonstrating the superior performance of the novel device. This comparison was carried out at the same inlet conditions for the vapor-air mixture and the coolant streams. Also, the streamwise temperature differences were similar in both cases. Further, the energy effectiveness of a three-stage bubble column dehumidifier was found to be similar to the conventional dehumidifier.

Improved Performance

This innovation reduces the heat-transfer area requirement to a fraction of that in existing HDH systems and is brought close to pure vapor levels (like multieffect desalination systems), as illustrated in Figure 15.

Therefore, by using thermal balancing and bubble column dehumidifiers, HDH system performance can be improved substantially, making such a system affordable for small-scale applications.

Acknowledgments

The authors would like to thank the King Fahd University of Petroleum and Minerals—Center for Clean Water and Clean Energy at MIT and KFUPM (project # R4-CW-08)—for funding the research reported in this article.

About the Authors

G. Prakash Narayan *(gpn@mit.edu) and* ***John H. Lienhard V*** *are with the Department of Mechanical Engineering, Massachusetts Institute of Technology, Cambridge, Mass.*

Footnote

[1]Dehumidifer name, George Fischer, city/state.

References

Annapoorania, A.; Murugesan, A.; Ramu, A.; and Renganathan, N.G., 2012. Groundwater quality assessment in coastal regions of Chennai City, Tamil Nadu, India, case study. Proceedings of India Water Week 2012—Water, Energy and Food Security, April 10–14, New Delhi.

Appello, T., 2006. Arsenic in ground water a global problem. Proceedings of Seminar Utrecht, Netherlands National Committee of IAH, J. P. Heedreik.

Bejan, A., 1996. *Entropy generation minimization: the method of thermodynamic optimization of finite size systems and finite time processes.* CRC Press, Boca Raton, Fla.

Bhuyan, B., 2010. A study on arsenic and iron contamination of groundwater in three development blocks of Lakhimpur District, Assam, India. *Report and Opinion*, 2:6:82–87.

Colburn, A.P. and Hougen, O.A., 1934. Design of cooler condensers for mixtures of vapors with noncondensing gases. *Industrial and Engineering Chemistry*, 26:1,178–1,182.

Denny, V.E.; Mills, A.F.; and Jusionis, V.J., 1971. Laminar film condensation from a steam-air mixture undergoing forced flow down a vertical surface. *Journal of Heat Transfer*, 93:297–304.

Denny, V.E. and Jusionis, V.J., 1972. Effects of noncondensable gas and forced flow on laminar film condensation. *International Journal of Heat and Mass Transfer*, 15:315–326.

Fawell, J.; Bailey, K.; Chilton, J.; Dahi, E.; Fewtrell, L.; and Magara, Y., 2006. Fluoride in drinking water. *WHO Drinking-water Quality Series*, IWA Publishing, London.

Hamieh, B.M.; Beckman, J.R.; and Ybarra, M.D., 2001. Brackish and seawater desalination using a 20 sq. ft. dewvaporation tower. *Desalination*, 140:217–226.

Hamieh, B.M. and Beckman, J.R., 2006. Seawater desalination using dewvaporation technique: experimental and enhancement work with economic analysis. *Desalination*, 195:14–25.

Hammond, A. 2007. *The next 4 billion: Market size and business strategy at the base of the pyramid.* World Resource Institute.

Hasanein, H.A., 1994. *Steam condensation in the presence of noncondensable gases under forced convection conditions.* PhD thesis, Massachusetts Institute of Technology.

Hasanein, H.A.; Kazimi, M.S.; and Golay, M.W., 1996. Forced convection in-tube steam condensation in the presence of noncondensable gases. *International Journal of Heat and Mass Transfer*, 39:2,625–2,639.

International Water Management Institute, 2007. *Water for food, water for life: A comprehensive assessment of water management.*

Joshi, J.B. and Sharma, M.M., 1979. A circulation cell model for bubble columns. *Chemical Engineering Research and Design*, 57a:244–251.

Kageyama, T.; Peterson, P.F.; and Schrock, V.E., 1993. Diffusion layer modeling for condensation in vertical tubes with noncondensable gases. *Nuclear Engineering and Design*, 141:289–302.

Kuhn, S.Z., 1995. *Investigation of heat transfer from condensing steam-gas mixture and turbulent films flowing downward inside vertical tubes.* PhD thesis, University of California at Berkeley.

Kulkarni, A.V. and Joshi, J.B., 2011. Design and selection of sparger for bubble column reactor, Part 1: Performance of different spargers. *Chemical Engineering Research and Design*, 89:1,972–1,985.

Maheshwari, N.K.; Vijayan, P.K.; and Saha, D., 2007. Effects of non-condensable gases on condensation heat transfer. Proceedings of Fourth RCM on the IAEA CRP on Natural Circulation Phenomena.

McGovern, R.K.; Thiel, G.P.; Narayan, G.P.; Zubair, S.M.; and Lienhard V, J.H., 2012 in press. Evaluation of the performance limits of humidification dehumidification desalination systems via a saturation curve analysis. *Applied Energy*.

Miller, J.A., 2011. *Numerical balancing in a humdification dehumidification desalination system.* Master's thesis, Massachusetts Institute of Technology.

Minkowycz, W.J. and Sparrow, E.M., 1966. Condensation heat transfer in the presence of noncondensables: interfacial resistance, superheating, variable properties, and diffusion. *International Journal of Heat and Mass Transfer*, 9:1,125–1,144.

Mistry, K.H.; Mitsos, A.; and Lienhard V, J.H., 2011. Optimal operating conditions and configurations for humidification–dehumidification desalination cycles. *International Journal of Thermal Sciences*, 50:779–789.

Narayan, G.P.; Lienhard V, J.H.; and Zubair, S.M., 2010a. Entropy generation minimization of combined heat and mass transfer devices. *International Journal of Thermal Sciences*, 49:2,057–2,066.

Narayan, G.P.; Sharqawy, M.H.; Lienhard V, J.H.; and Zubair, S.M., 2010b. Thermodynamic analysis of humidification dehumidification desalination cycles. *Desalination and Water Treatment*, 16:339–353.

Narayan, G.P; Sharqawy, M.H.; Summers, E.K.; Lienhard V, J.H.; Zubair, S.M.; and Antar, M.A., 2010c. The potential of solar-driven humidification-dehumidification desalination for small-scale decentralized water production. *Renewable and Sustainable Energy Reviews*, 14:1,187–1,201.

Narayan, G.P.; Mistry, K.H.; Sharqawy, M.K.; Zubair, S.M.; and Lienhard V, J.H., 2010d. Energy effectiveness of simultaneous heat and mass exchange devices. *Frontiers in Heat and Mass Transfer*, 1:1–13.

Narayan, G.P.; Chehayeb, K.M.; McGovern, R.K.; Thiel, G.P.; Lienhard V, J.H.; and Zubair, S.M., under review. Thermodynamic balancing of the humidification dehumidification desalination system by mass extraction and injection. *International Journal of Heat and Mass Transfer*.

Narayan, G.P.; Sharqawy, M.H.; Lam, S.; and Lienhard V, J.H., 2012. Bubble columns for condensation at high concentrations of non-condensable gas: heat transfer model and experiments. *AIChE Journal,* volume: issue: pages.

Narayan, G.P.; Thiel, G.P.; McGovern, R.K.; Sharaqawy, M.H.; and Lienhard V, J.H., 2011. Vapor-mixture condenser. US Patent filing no. USSN 13/241,907.

Nusselt, W., 1916. Die oberflachenkondensation des wasserdampfes. *Zeitschrift des Vereins-DeutscherIngenieure*, 60:541–546.

Prahalad, C.K. and Hammond, A., 2002. Serving the world's poor profitably. *Harvard Business Review*, 2002:4–11.

Rao, V.D.; Krishna, V.N.; Sharma, K.V.; and Rao, P.M., 2008. Convective condensation of vapor in the presence of a non-condensable gas of high concentration in laminar flow in a vertical pipe. *International Journal of Heat and Mass Transfer*, 51:6,090–6,101.

Sauvet-Goichon, B., 2007. Ashkelon desalination plant—a successful challenge. *Desalination*, 203:75–81.

Siddique, M.; Golay, M.W.; and Kazimi, M.S., 1992. Local heat transfer coeffcients for forced convection condensation of steam in a vertical tube in the presence of air. T*wo-Phase Flow and Heat Transfer*, third edition, 197:386–402, ASME, New York.

Sievers, M., 2010. *Design and optimization of a dehumidifier in a humidification-dehumidification (hdh) desalination system*. Master's thesis, Technische Universtat Hamburg-Harburg.

Sparrow, E.M. and Eckert, E.R.G., 1961. Effects of superheated vapor and noncondensable gases on laminar film condensation *AIChE Journal*, 7:473–477.

Sparrow, E.M.; Minkowycz, W.J.; and Saddy, M., 1967. Forced convection condensation in the presence of noncondensables and interfacial resistance. *International Journal of Heat and Mass Transfer*, 10:1,829–1,845.

Thiel, G.P. and Lienhard V, J.H., 2012. Entropy generation in condensation in the presence of high concentrations of noncondensable gases. *International Journal of Heat and Mass Transfer*, 55:5,133–5,147.

United Nations, 2003. Water for people, water for life, executive summary, Water Development Report.

United Nations, 2008. The millennium development goals report, Tech. Rep., New York.

Wang, C.Y. and Tu, C.J., 1988. Effects of non-condensable gas on laminar film condensation in a vertical tube. *International Journal of Heat and Mass Transfer*, 31:2,339–2,345.

Editor's Note

This is an updated, peer-reviewed version of a paper presented at IDA World Congress 2011, Sept. 4–9, Perth, Western Australia.